Progress in the Study on the Formation of the Summertime Subtropical Anticyclone

LIU Yimin* (刘屹岷) and WU Guoxiong (吴国雄)

State Key Laboratory of Numerical Modeling for Atmospheric Sciences and Geophysical Fluid Dynamics, Institute of Atmospheric Physics, Chinese Academy of Sciences, Beijing 100029

(Received 15 August 2003; revised 6 March 2004)

ABSTRACT

The studies in China on the formation of the summertime subtropical anticyclone on the climate timescale are reviewed. New insights in resent studies are introduced. It is stressed that either in the free atmosphere or in the planetary boundary, the descending arm of the Hadley cell cannot be considered as a mechanism for the formation of the subtropical anticyclone. Then the theories of thermal adaptation of the atmosphere to external thermal forcing and the potential vorticity forcing are developed to understand the formation of the subtropical anticyclone in the three-dimensional domain. Numerical experiments are designed to verify these theories. Results show that in the boreal summer, the formation of the strong South Asian High in the upper troposphere and the subtropical anticyclone over the western Pacific in the middle and lower troposphere is, to a great extent, due to the convective latent heating associated with the Asian monsoon, but affected by orography and the surface sensible heating over the continents. On the other hand, the formation of the subtropical anticyclone at the surface over the northern Pacific and in the upper troposphere over North America is mainly due to the strong surface sensible heating over North America, but affected by radiation cooling over the eastern North Pacific. Moreover, in the real atmosphere such individual thermal forcing is well organized. By considering the different diabatic heating in synthesis, a quadruple heating pattern is found over each subtropical continent and its adjacent oceans in summer. A distinct circulation pattern accompanies this heating pattern. The global summer subtropical heating and circulation may be viewed as "mosaics" of such quadruplet heating and circulation patterns respectively. At last, some important issues for further research in understanding and predicting the variations of the subtropical anticyclone are raised.

Key words: subtropical anticyclone, quadruplet heating, mosaic circulation

1. Introduction

Along the subtropics of the Northern and Southern Hemispheres, there exist belts of the subtropical anticyclone. There are two pronounced anticyclones near the surface in the boreal summer. One is the sea surface subtropical anticyclone over the western North Pacific (SAWP), and the other is the subtropical anticyclone over the North Atlantic (SANA). The SAWP alone covers about twenty to twenty five percent of the northern globe. In the free atmosphere in the boreal summer, the circulation over East Asia is characterized by the existence of two persistent subtropical anticyclone systems. One is the remarkable South Asian anticyclone (SAA) in the upper troposphere just over the region to the north of the Bay of Bengal; and the other is the SAWP in the middle and lower troposphere. The seasonal variations of these two systems are closely linked to the onset and withdrawal of the Asian summer monsoon (Tao, 1963; Tao and Chen, 1987). Their spatial and temporal variations are associated not only with the disastrous weather events in the area, such as typhoons and torrential rains, but also with severe climate anomalies, such as drought and flooding over vast areas (Tao and Xue, 1962). Ye and Zhu (1958) and Ye et al. (1958) found that the abrupt northward movement from winter to summer of the subtropical anticyclone in the Asian monsoon area is accompanied with abrupt changes in circulation patterns. Tao (1963), Tao and Xue (1962), and Tao et al. (1962), Huang and Yu (1962), and Huang (1963) studied the

*E-mail: lym@lasg.iap.ac.cn

SAWP and revealed its seasonal variation in intensity, structure, and location, and its structure in association with the distribution of summer rainfall in China. As a matter of fact, the activities of the SAWP are also closely linked with the weather and climate anomalies in Korea and Japan (e.g., Kurihara and Tsuyuki, 1987; Kurihara, 1989; Nikaidou, 1988). Many factors have also been proposed to explain the variation and formation of the subtropical anticyclone as reviewed by Liu and Wu (2000). These include the circulation interactions (Tao and Zhu, 1964), the impact of the Tibetan Plateau (Krishnamurti et al., 1973; Ye and Gao, 1979; Wu and Zhang, 1998; Ye and Wu, 1998), etc. In recent years, the influence of the East Asian monsoon and sea surface temperature anomaly on the formation and variation of subtropical anticyclones (Li and Luo, 1988; Yu and Wang, 1989; Nikaidou, 1989; Qian and Yu, 1991; Hoskins, 1996; Wu et al., 1999; Liu et al., 1999b, 2001, 2002; Rodwell and Hoskins, 2001) has also been emphasized.

However, due to the limitations in available data and development of our sciences, by early 1990's, the mechanism of the subtropical anticyclone formation was still unclear, and its forecast is still unsatisfactory. By the mid 1990s, the NCEP/NCAR reanalysis data set (Kalnay et al., 1996) became available, and a climate system model of the Global Ocean Atmosphere Land System (GOALS model) that had coupled the three climate sub-systems together was completed (Wu et al., 1997b; Zhang et al., 2000). To advance our understanding of the subtropical anticyclone, in 1995 the National Natural Science Foundation of China (NSFC) decided to set up a Key Project entitled "The formation and variation of the subtropical anticyclone". Since then, many new research results have been obtained. They show that it is due to the diabatic heating, instead of the descending arm of the Hadley cell, that the summertime subtropical anticyclones are formed. The material presented here provides a summary of the research results. In section 2, after introducing the general concepts and dynamics of the zonal mean subtropical anticyclone, the contrasts in observation as well as dynamics between the local subtropical anticyclones and meridional circulations over the western and eastern Pacific are made. In section 3, some relevant dynamics are presented for understanding the three-dimensional features of the subtropical anticyclone. The effects of the surface sensible heating, deep convective condensation heating, and radiation cooling are discussed in sections 4 to 6, respectively. Since these results indicate that different diabatic heatings play different roles in the formation of subtropical anticyclones and should be considered in synthesis, section 7 employs the reanalysis data of NCEP/NCAR to demonstrate the distributions of individual as well as total diabatic heatings against circulations in the summer subtropics. Discussions and conclusions are presented in section 8.

2. Distributions of the subtropical high and the Hadley cell

In this section, several criteria are proposed to compare the distributions of the local subtropical anticyclones against the meridional circulations at the longitudes 135°E and 125°W over the western and eastern Pacific, respectively.

2.1 *General concepts of the subtropical anticyclone*

In the free atmosphere the zonal mean flow can be described by using the geostrophic relation, and the equation of the divergence of meridional mass flux $(\partial(\rho v)/\partial y)$ in a steady state can be obtained as

$$\frac{\partial(f\rho u)}{\partial y} + \frac{\partial^2 p}{\partial y^2} = 0\,, \tag{1}$$

where ρ is air density, p is pressure, and the other symbols used here are conventional in meteorology. Equation (1) implies that under the constraint of the geostrophic relation, the convergence of mass flux due to the exertion of the Coriolis force upon the zonal flow $(\partial(-f\rho u)/\partial y < 0)$ is balanced by the divergence of mass flux produced by the pressure gradient force $(-\partial^2 p/\partial y^2 > 0)$, as depicted schematically in Fig. 1a.

Within the planetary boundary layer, friction impacts need to be considered and equation (1) is modified as

$$\frac{\partial(f\rho u)}{\partial y} + \frac{\partial^2 p}{\partial y^2} = -\frac{k\partial(\rho v)}{\partial y}\,, \tag{2}$$

where k is a friction coefficient. Thus the surface subtropical anticyclone is accompanied with a strong horizontal divergence of mass flux $(\partial(\rho_0 v)/\partial y > 0)$ within the boundary layer. Since the mass transport into the boundary layer at the top D_e of the Ekman layer is equal to the divergence of the cross-isobaric mass transport in the layer, i.e.,

$$\rho_0 w(D_e) = -\frac{\partial}{\partial y}\int_0^{D_e} \rho_0 v dz\,, \tag{3}$$

the location of the subtropical anticyclone within the planetary boundary layer is then characterized by atmospheric descent at the top of the Ekman layer. Traditionally, the atmospheric descent is considered as a mechanism for the formation of the subtropical anticyclones. However, results from (2) and (3) show that this consideration is inappropriate since such a descent is a result of divergence along the ridgeline in

the planetary boundary layer. Both the descent and the cross-isobaric flow in association with the anticyclone are secondary non-divergence circulations, and do not contribute to the mass build-up in the layer, as depicted schematically in Fig. 1b. It is the inertial effect of the earth's rotation that causes the mass accumulation along the boundary between the westerly in the mid-latitudes and the easterly in the tropics, forming surface high pressure along the subtropics, as in the free atmosphere.

2.2 *Location and intensity of the subtropical anticyclone*

The meridional wind component vanishes at the latitude where the zonal mean center of the subtropical anticyclone is located. Thus in both the free atmosphere and the planetary boundary layer, the location of the ridge of the subtropical anticyclone in the sense of zonal mean can be defined from the zonal wind distribution by using the following criteria:

$$\begin{cases} \text{(a) } u = 0 \text{ ;} \\ \text{(b) } \partial u/\partial y \begin{cases} > 0 \text{ , in the Northern Hemisphere ,} \\ < 0 \text{ , in the Southern Hemisphere .} \end{cases} \end{cases} \tag{4}$$

The vertical variation in the location of the subtropical anticyclone can be understood by using the thermal wind relation:

$$\partial u/\partial p = (\alpha/f\theta)\partial\theta/\partial y \text{ .} \tag{5}$$

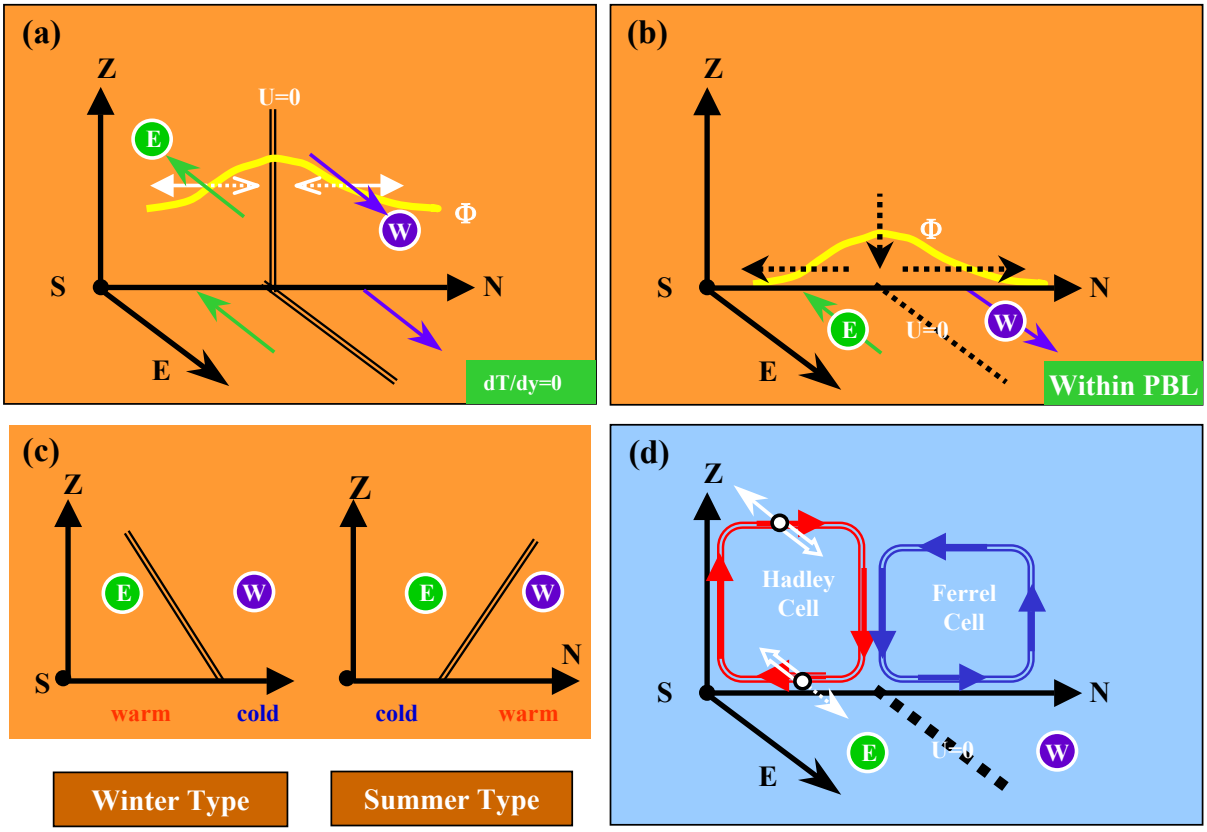

Fig. 1. Schematic diagram showing the dynamic mechanism for the maintenance of the zonal mean subtropical anticyclone and the meridional Hadley cell. (a) In the north-south direction at the ridgeline of the subtropical anticyclone, the convergence of meridional mass flux owing to the inertial effects of the Earth's rotation ($-f$, dotted arrow) is balanced by its divergence due to the pressure gradient force ($-\nabla\Phi$, solid white arrow). (b) In the planetary boundary layer, the cross-isobaric flow that diverges from the subtropical anticyclone outwards is balanced by the descent at the top of the planetary boundary layer into the layer. (c) According to the thermal wind relation, the ridge of the subtropical anticyclone tilts with increasing height towards the warmer region, forming westerly shear in winter and easterly shear in summer crossing the ridgeline upwards in the Asian monsoon area. (d) The inertial torques associated with the horizontal branches of the Hadley Cell (blank white arrow) are balanced by the generation of angular momentum due to friction at the surface (dotted arrow), and by the divergence of angular momentum from the tropics to mid-latitudes in the upper troposphere (solid arrow).

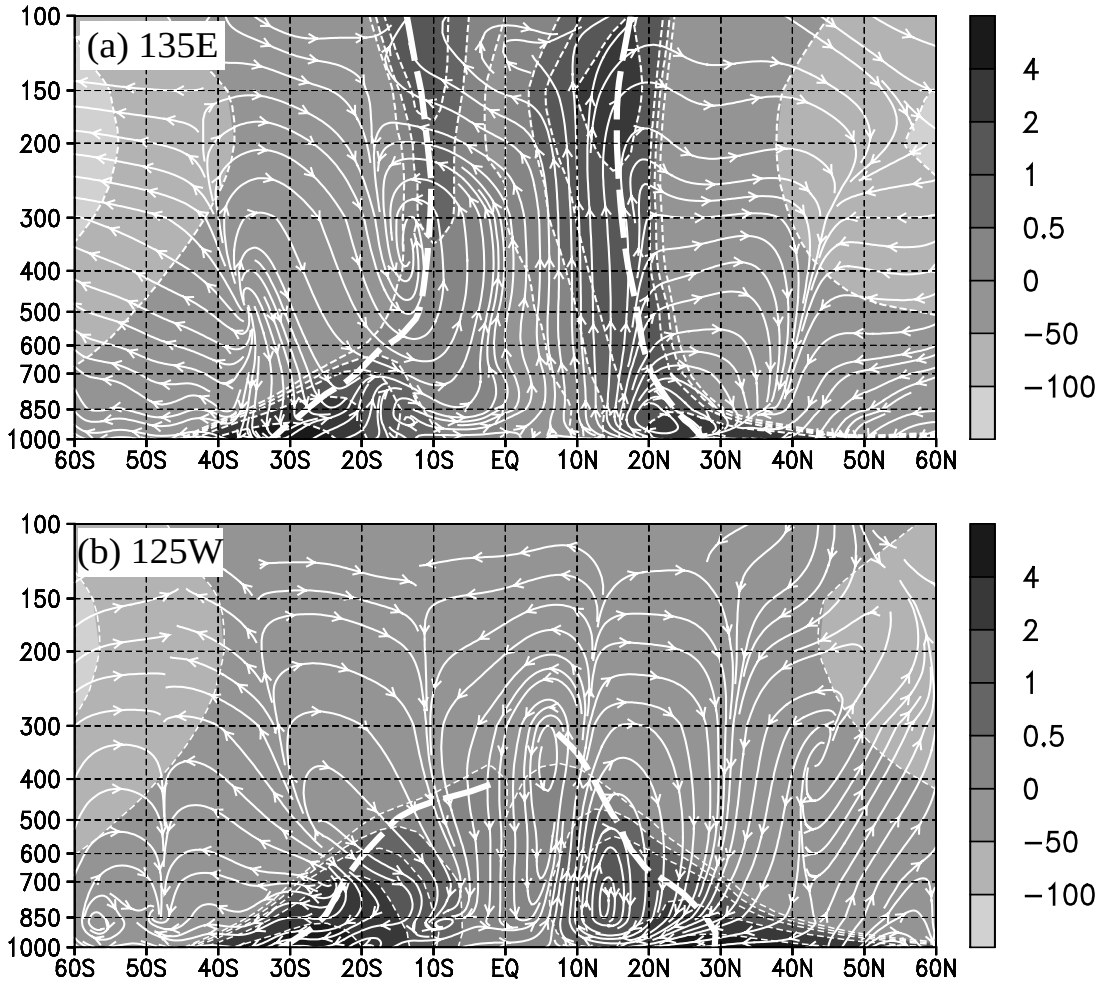

Fig. 2. Annual mean distributions averaged from 1980 to 1997 of the meridional deviation of geopotential height from its equatorial value at the same level (shading, units: 10 gpm), the meridional circulations (light streamline with vectors), and the ridgeline of the subtropical anticyclone identified by the curve $u = 0$ (heavy dashed curve) along (a) 135°E and (b) 125°W.

For simplicity, the p-coordinate is adopted in (5), in which θ is potential temperature and α, the specific volume of the air. Equation (5) means the ridgeline of the subtropical anticyclone tends to tilt towards warmer latitudes with increasing height (Fig. 1c). Thus in the Asian monsoon region in the boreal summer, there should be easterly shear upwards across the ridgeline when the land surface of the southern part of Asia gets warmer than the sea surface of the North Indian Ocean (Mao et al., 2002).

The intensity of the subtropical anticyclone (I) can be measured by the convergence or accumulation of the meridional mass flux

$$I = \partial(f\rho u)/\partial y = f\rho\partial u/\partial y + \rho u\beta\,. \qquad (6)$$

Here, β is the meridional gradient of Coriolis parameter f, and density is assumed to be independent of y in the vicinity of the ridgeline of the subtropical anticyclone. Formula (6) together with (1) implies that the intensity of the subtropical anticyclone can be measured by $-\partial^2 p/\partial y^2$. Furthermore, in p-coordinates this is equivalent to $-\rho\partial^2\Phi/\partial y^2$. For simplicity $-\partial^2\Phi/\partial y^2$ or geopotential height Φ can also be used as an intensity index.

2.3 *Distribution of the subtropical anticyclone and meridional circulation*

Wu et al. (2002) have shown that in the zonal and annual mean case, the descending arm of the Hadley circulation and the subtropical anticyclone deviate from each other in the free atmosphere, and coincide only in the planetary boundary layer. In their study, the deviation $\phi(y, p)$ of the geopotential height ($\Phi(y, p)$) at latitude y and at pressure level p from its value at the equator ($y = 0$) and at the

same level ($\Phi(0,p)$), i.e., $\phi(y,p)=\Phi(y,p)-\Phi(0,p)$, was used to present the distributions of the subtropical anticyclone. The advantage of using such a deviation of geopotential height is that, by removing the large amount $\Phi(0,p)$ that is irrelevant to our present study, the much smaller deviation field $\phi(y,p)$ can demonstrate the three-dimensional structure of the subtropical anticyclone much more clearly (Liu, 1999). By using this scheme, the annual mean climate distributions of $\phi(y,p)$ along 135°E and 125°W are plotted in Fig. 2 versus the in situ meridional circulations. It is prominent that the isopleth $u=0$ coincides almost everywhere with the maximum $\phi(y,p)$ at the same level, and criteria (4) is adequate in defining the location of the subtropical anticyclone even in the local sense. As in the zonal mean case (Wu et al., 2002), the two ridgelines in the two hemispheres are approximately symmetric about the equator. In Fig. 2, a significant difference between the two hemispheres in the domain of positive geopotential height deviation can be observed below 500 hPa. Particularly at 1000 hPa along 125°W, although its poleward rim in the Southern Hemisphere is bounded by 44°S, in the Northern Hemisphere it extends northward to approach 60°N. This can be attributed to the existence of the strong surface subtropical anticyclone over the Northeast Pacific in the boreal summer.

The deviation fields $\phi(y,p)$ along the ridgelines in the two hemispheres are approximately symmetric about the equator, and decrease with increasing height below 700 hPa. They are over 40 gpm at the surface with centers located at 30°, but about 10–20 gpm at 700 hPa near 20°. In this layer, the ridgelines in the two hemispheres both tilt equatorward with increasing height. The weakening in intensity of the subtropical anticyclone with increasing height is in accordance with the equator ward tilting of its ridgeline. This is because as the ridgeline is approaching the equator with increasing height, the Coriolis parameter and air density both become smaller. According to (6), for the same zonal wind shear, there is less convergence of mass flux along the ridgeline, leading to the weakening in intensity. Above 300 hPa along 135°E, the deviation increases with height in the two hemispheres, in accordance with their poleward tilting.

Traditionally, the formation of the subtropical anticyclone is attributed to the dynamic effects of the subsidence of the sinking arm of the Hadley circulation. To verify this hypothesis, Fig. 2 also shows the meridional circulations. It is apparent that the sinking arms of the local meridional cells do not coincide with the subtropical anticyclone except at the surface, where the ridgeline of the surface subtropical anticyclone is always accompanied with vertical descent. Along 135°E (Fig. 2a) above 700 hPa, the ridgelines of the subtropical anticyclones in the two hemispheres are located between 10° and 20°. The strongest descending branch in the Northern Hemisphere is located by 40°N to the north of the ridgeline, whereas in the Southern Hemisphere it is located around 15°S to the south of the ridgeline of the southern subtropical anticyclone. Over the eastern Pacific along 125°W (Fig. 2b), the descending arm of the local meridional circulation in the Northern Hemisphere is vertically located around 30°N, whereas in the Southern Hemisphere it is located around 10°S. It is clearly seen from Fig. 2 that the distributions of the subtropical anticyclones and the descending arms of the meridional circulation are not in coordination in the free atmosphere either over the western Pacific (Fig. 2a) or over the eastern Pacific.

As stated by Eady (1949) and Kuo (1956), the mean meridional circulation is forced only when the geostrophic and hydrostatic balances are destroyed by diabatic heating and/or eddy transfer of heat and momentum. The generation of the mean meridional circulation in return is to restore new geostrophic and hydrostatic balances. As long as the conservation of angular momentum is concerned, as shown in Fig. 1d the positive inertial torque ($f\rho v$) of the upper branch of the Hadley cell balances the eddy transfer of angular momentum from the tropics to higher latitudes to maintain the subtropical jet (Held and Hou, 1980); whereas the negative inertial torque of its lower branch balances the positive surface frictional torque that is negatively proportional to the surface easterly zonal wind (Wu, 1988). From the above discussions, we see the contrast in the formation dynamics between subtropical anticyclone and Hadley circulation. The formation of the subtropical anticyclone is associated with the convergence or accumulation of meridional mass flux. This can be understood by employing the v-momentum equation. Although the vertical tilting of the ridgeline of the subtropical anticyclone is determined by the thermal structure of the atmosphere, the ultimate forcing of the formation of the subtropical anticyclone is the rotation of the earth. On the other hand, the Hadley circulation is thermally driven. Its maintenance mechanism includes the requirement of the conservation of angular momentum that can be understood by using the u-momentum equation. In the planetary boundary layer, it is also the inertial impact of the earth's rotation that forms the surface subtropical anticyclone. Due to the surface frictional

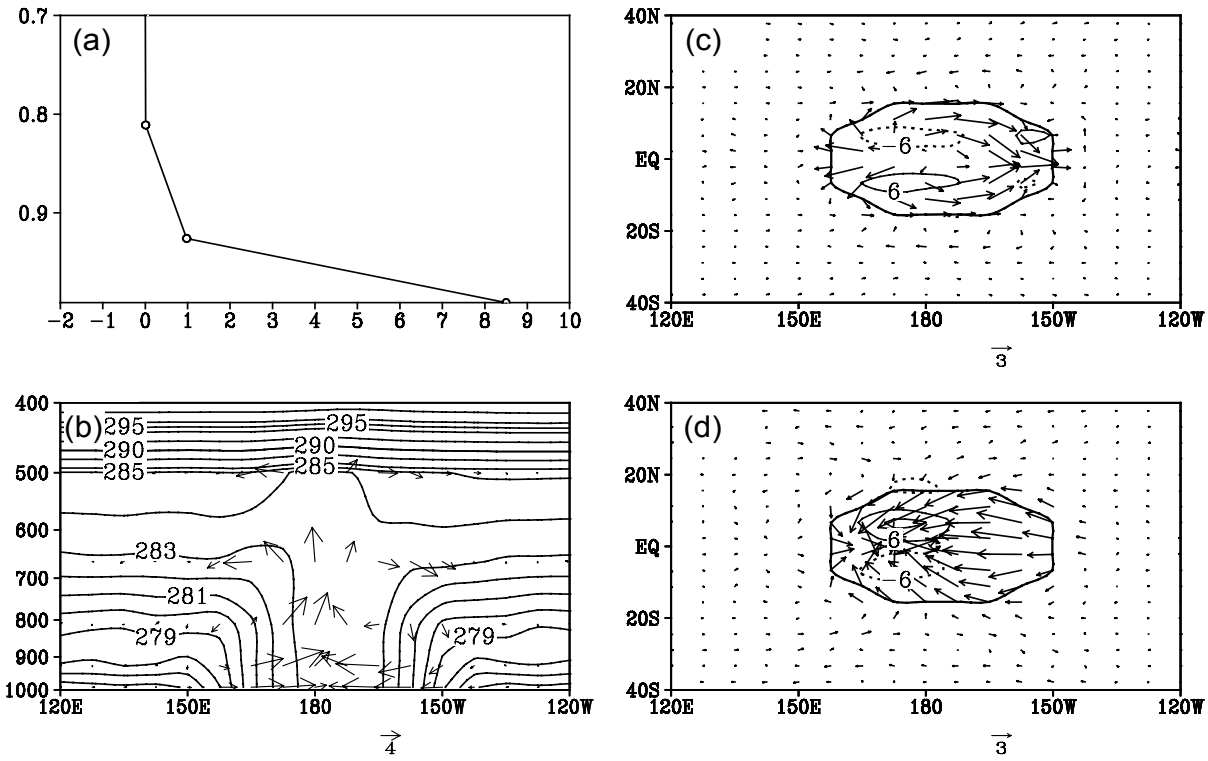

Fig. 3. Numerical experiment on the thermal adaptation of the atmospheric flow field and vorticity field (10^{-6} s^{-1}) to a prescribed surface sensible heating at Day 3 and at the upper level $\sigma = 0.664$ (c) and lower level $\sigma = 0.991$ (d). (a) The heating rate (K d^{-1}) at Day 3. Solid and dashed curves denote positive and negative values respectively, and the heavy solid curve bounds the heating region which is more than 1 W m^{-2}. (b) Vertical cross sections at the equator of potential temperature (K) and velocity (units: u in m s^{-1}, ω in -40 Pa s^{-1}) at Day 3. (adopted from Wu and Liu, 2000).

dissipation, there is mass divergence along the ridgeline of the surface subtropical anticyclone in the planetary boundary layer. This is compensated for by the descending mass flow at the top of the planetary layer. Therefore the surface subtropical anticyclone must be accompanied with the in situ atmospheric descent. Such descent, however, does not contribute to the mass build-up along the surface high. In other words, the descent at the surface subtropical high is a result of the surface high.

The above discussions do not mean that the formations of the subtropical anticyclone and the Hadley circulations are separated. Although the subtropical anticyclone exists because of the meridional mass flux convergence due to Coriolis turning, the existence of the zonal mean tropical easterlies and midlatitude westerlies in the first place is closely associated with the Hadley cell. The simple Hadley cell model of Held and Hou (1980) clearly shows that the Hadley circulation must exist at least within the subtropics in order to maintain the zonal winds and an associated temperature field consistent with angular momentum conservation. This model produces a westerly jet at the subtropical tropopause and a surface easterly in the tropics. The ridgeline of the subtropical anticyclone defined by $u = 0$ then tilts equatorward (their Fig. 3) following the thermal wind relation. It is therefore separated from the descending arm of the Hadley cell and located to the equatorward side of the descending arm, as is observed from Fig. 2 and represented in Fig. 1d.

3. Thermal adaptation and PV (potential vorticity)-forcing

In the Northern Hemisphere in winter, westerlies dominate the mid-latitudes and subtropics in the upper troposphere. Mountain forcing plays an important role in the formation of the circulation patterns (Charney and Elliason, 1949; Bolin, 1950; Yeh, 1950; Rodwell and Hoskins, 2001). On the other hand in the summer subtropics, the upper tropospheric westerly is weak, and thermal forcing becomes more important in influencing the circulation and in the forma-

tion of the subtropical anticyclones. Before we discuss the formation of subtropical anticyclones in the three-dimensional domain, in this section we show through numerical experiments how the atmosphere responds to a given thermal forcing.

3.1 *Numerical experiments about thermal adaptation*

The adaptation of atmospheric circulation to external diabatic heating can be understood through the PV-θ view, according to which a heating (cooling) can produce lower layer cyclonic (anticyclonic) vorticity and upper layer anticyclonic (cyclonic) vorticity (Hoskins, 1991; Wu and Liu, 2000). In the current section, numerical experiments are designed to examine this thermal adaptation theory.

The model used is the GOALS model which is developed at State Key Lab of Atmospheric Sciences and Geophysical Fluid Dynamics (LASG), Institute of Atmospheric Physics (IAP) (Wu et al., 1997b; Zhang et al., 2000) and has participated in the Atmospheric Model Inter-comparison Program (AMIP), the Coupled Model Inter-comparison Program (CMIP), and Task I of the Intergovernmental Panel on Climate Change (IPCC, 2001). The atmosphere component GOALS_AGCM (Wu et al., 1996) has nine levels in the vertical and is rhomboidally truncated at wave number 15 in the horizontal. The ocean component (Zhang et al., 1996) has 20 layers in the vertical with a horizontal resolution of 4° degree latitude by 5° longitude. The land component uses the SSiB model (Xue et al., 1991; Liu and Wu, 1997). The K-distribution scheme developed by Shi (1981) is employed for presenting the radiation processes.

For the present purpose, the ocean and land components are switched off, and an aqua-planet is assumed. The climate July- and zonal- mean sea surface temperature is imposed as the lower boundary condition. The solar angle is fixed by its value on 15 July. Other variables, including CO_2, aerosol, cloud amount, and atmospheric variables, all assume their corresponding July zonal means. The initial wind and the horizontal gradient of temperature $\nabla_h T$ are set to zero. For simplicity, an axially symmetric surface heating source is imposed at the equator. The intensity of the heating source is 100 W m^{-2} at the center, and decreases gradually towards the boundary (Fig. 3). The setting of 100 W m^{-2} for the experiment is in reference to the observations that over equatorial Africa and Latin America, the surface sensible heat flux in July is commonly above this value. To concentrate on the atmospheric response to such an imposed surface diabatic heating, condensation heating and the sensible heating over other parts of the world are switched off from the thermodynamic equation.

The maximum vertical distribution of diffusive sensible heating over the heating region is located at about 920 hPa, with an intensity of 8 K d^{-1} on Day 3. The heating decreases with height and approaches zero near 800 hPa. Figure 3d presents the wind and vorticity fields at the $\sigma = 0.991$ level. The diabatic heating results in cyclonic vorticity and horizontal convergence in the lower layer, but anticyclonic circulation and divergence at the upper level of $\sigma = 0.664$ (Fig. 3c). The vorticity is on the order of 10^{-6} s^{-1} outside the equator. The isentropic surfaces become concave after one day of heating (Fig. 3b). Air converges in the lower layer, penetrates the isentropic surfaces over the heating region, and diverges at the upper level of $\sigma = 0.664$. All these results agree with the theoretical analysis (Wu and Liu, 2000). In another experiment in which the center of the surface sensible heating is located at 35°N, similar results are obtained (Figs. 3.11–3.14 in Liu, 1998) except that the asymmetric Gill-type circulation is also induced. The symmetric subtropical anticyclone belt is then broken, and enclosed anticyclone systems are formed. These will be investigated further in section 4.

3.2 *PV-forcing and the subtropical anticyclone*

The flux form of the potential vorticity equation is

$$\frac{DW}{Dt} = \boldsymbol{F}_\zeta \cdot \nabla\theta + \boldsymbol{\zeta}_a \cdot \nabla Q \,, \tag{7}$$

where, $\boldsymbol{F}_\zeta = \nabla \times \boldsymbol{F}$, and $\boldsymbol{F}$ is the frictional force per unit mass contained in the three-dimensional momentum equation, $\boldsymbol{\zeta}_a$ is the three-dimensional absolute vorticity, and

$$W = \boldsymbol{\zeta}_a \cdot \nabla\theta \,.$$

Based on scale analysis, the relation between diabatic heating Q and the forced atmospheric circulation along the subtropics and at a steady state can be expressed as (Liu et al., 1999a, 1999b, 2001)

$$\boldsymbol{V} \cdot \nabla\zeta + \beta v \approx \theta_z^{-1}(f+\zeta)Q_z$$
$$\left(\theta_z = \frac{\partial\theta}{\partial z} \neq 0 \,,\ \ Q_z = \frac{\partial Q}{\partial z}\right) \,. \tag{8}$$

A similar relation to (8) at a steady state can also be obtained by combining the approximated thermodynamic equation

$$w \approx Q\theta_z^{-1} \,, \quad \theta_z \neq 0 \,,$$

and the vorticity equation

$$\boldsymbol{V} \cdot \nabla\zeta + \beta v = f\frac{\partial w}{\partial z} \,.$$

In the lower troposphere in the summer subtropics, or in the troposphere during deep convection occasions,

the vorticity advection is weak, and (8) can be further simplified to the following Sverdrup balance:

$$\beta v \approx \theta_z^{-1}(f+\zeta)Q_z\ ,\ \ (\theta_z \neq 0)\ . \tag{9}$$

This implies that the thermally forced circulation along the subtropics depends strongly on the vertical profile of the heating. Since f is positive in the Northern Hemisphere but negative in the Southern Hemisphere, for a statically stable atmosphere, a heating which increases with altitude then generates poleward flow, whereas a heating which decreases with altitude produces equatorward flow. This then provides another base for understanding the formation of the subtropical anticyclones in summer.

3.3 *Subtropical anticyclone forced by surface sensible heating*

During boreal summer along the subtropics, land-surface sensible heat flux usually exceeds 100 W m^{-2}, which amounts to a heating rate (Q) of 10^{-5} K s^{-1}. For a large-scale atmospheric system such as the subtropical anticyclone, the order of magnitude for θ_z is estimated as $\theta_z \sim 10^{-2}$ K m^{-1}. Then the orders of magnitude of the forcing terms on the right-hand sides of (8) and (9) are estimated to be 10^{-10} s^{-2} (Liu et al., 1999a). Following the discussions presented by Haynes and McIntyre (1987), Hoskins (1991), and Wu and Liu (2000), such strong surface heating will generate a cyclone at the surface and an anticyclone aloft (lower part of Fig. 4a). At the same time, since the maximum sensible heating appears near the land surface, Q_z is negative. According to (9), the forced northerly in the lower layers is estimated to 10^0 m s^{-1}. This means that, in response to a surface sensible heat flux of 100 W m^{-2}, the equatorward winds of several m s^{-1} will be forced over the heating region in the lower layers with a thickness of about one kilometer. The symmetric subtropical flow is then interrupted, and the lower layer anticyclone is forced to the west of the heating region, as shown schematically in the middle part of Fig. 4a.

In the upper layers in the subtropics, due to vertical westerly wind shear, zonal advection of vorticity overwhelms the β-effect, and (8) can be approximated as

$$\partial\zeta/\partial x \approx (f+\zeta)u^{-1}Q_z\theta_z^{-1} < 0,\ \ (\theta_z \neq 0)\ . \tag{10}$$

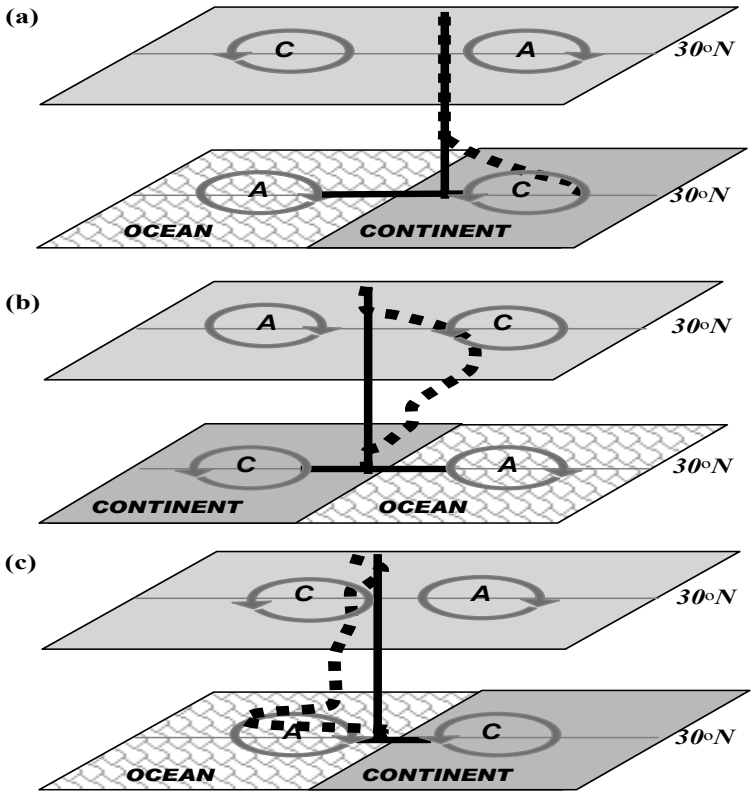

Fig. 4. Schematic diagram indicating the summertime subtropical atmospheric response to the vertically differential diabatic forcing of (a) sensible heating, (b) deep condensation heating, and (c) longwave radiative cooling. "A" denotes anticyclone, "C" denotes cyclone, and the profiles at the centers of each panel indicate the dominant heating.

For a heating scale of 10^6–10^7 m, and a westerly flow of 10^1 m, a negative relative vorticity of the order of 10^{-5} s^{-1} should appear downstream of the westerlies, contributing to the formation of the downstream subtropical anticyclone, as is shown schematically by the upper part of Fig. 4a.

3.4 *Subtropical anticyclone forced by deep convective condensation heating*

Along the subtropics, maximum latent heating associated with deep convection usually occurs at a height $Z_{\rm M}$ between 300 and 400 hPa, where the heating rate due to condensation can be estimated as Q$\sim 10^{-4}$ K s^{-1}. Using (9), the order of magnitude of the diabatic term $\theta_z^{-1}(f+\zeta)Q_z$ is also 10^{-10} s^{-2} below the maximum heating layer ($z = Z_{\rm M}$), but 10^{-9} s^{-2} above this layer. However, unlike in the case of sensible heating, the large latent heating rate of 10^{-4} K s^{-1} at $z = Z_{\rm M}$ results in strong westerlies to its north and easterlies to its south. Thus, even in the upper troposphere in the subtropics, vorticity advection above a deep convection area is usually small. The response of the atmosphere to deep convective latent heating can then be approximated to

$$v \approx (f+\zeta)\beta^{-1}Q_z\theta_z^{-1}\begin{cases} <0 & (z > Z_{\rm M}) \\ >0 & (z < Z_{\rm M}) \end{cases} \quad (\theta_z \neq 0)\ . \tag{11}$$

Thus the southerly is forced below $Z_{\rm M}$, while the northerly is forced in the upper troposphere. Therefore, in the upper troposphere, the subtropical anticyclone is formed to the west of the deep convection region as shown in the upper part of Fig. 4b, while the lower tropospheric subtropical anticyclone is formed to its east as shown in the middle part of Fig. 4b. Yet, cyclonic circulation near the surface is generated due to the atmospheric thermal adaptation to condensational heating as in the case of sensible heating (lower part of Fig. 4b).

3.5 *Subtropical anticyclone forced by longwave radiative cooling*

In summer in the subtropics, radiative cooling overwhelms the heating over the eastern oceans and on the poleward side of the western oceans (Wu and Liu, 2003). In particular, it is stronger than 100 W m^{-2} over the eastern coastal region of each ocean basin. The maximum longwave radiative cooling (LO) is usually below 850 hPa with an intensity of about –6 K d^{-1}. Following a similar argument, such radiative cooling can produce a vorticity forcing of $+10^{-10}$ s^{-2} in the upper troposphere and -10^{-9} s^{-2} in the lower troposphere. Poleward flow of several m s^{-1} in the upper layer and stronger equatorward flow in the lower troposphere are then forced. Such radiation-induced meridional flows reinforce those circulation patterns generated by sensible heating (Fig. 4a), and favor the formation of the subtropical anticyclone to the west of the radiative cooling in the lower troposphere but to its east in the upper troposphere, as shown in Fig. 4c. We may therefore propose that the strong negative vorticity forcing near the surface due to LO over the eastern oceans contributes to the eastward shift of the surface oceanic subtropical anticyclone, resulting in the asymmetric configuration of the surface subtropical anticyclones over the oceans.

4. Sensible heating and subtropical anticyclones over the North Pacific and North America

To see the relative importance of the vorticity advection and β-effect in the formation of the subtropical anticyclones over the Northwestern Pacific and North America in the lower troposphere, the NCEP/NCAR reanalysis data from 1980 to 1995 are retrieved to evaluate the terms shown in (8). Panels (a) and (b) in Fig. 5 show, respectively, the July mean distributions of the zonal asymmetric geopotential height at 1000 hPa and 500 hPa. At the surface over the northern Pacific (Fig. 5a), a positive center of more than 90 gpm is found to the west of North America. At 500 hPa the positive center is above North America (Fig. 5b), just downstream of the maximum vorticity forcing as shown in (Fig. 5d). The distributions in the region of the surface sensible heat flux and the resultant vorticity forcing near the surface are shown in panels (Fig. 5c) and (Fig. 5d). It is prominent that the July surface sensible heat flux over the oceans is weak, and its maximum appears along the western coast of North America, with an intensity of about 150 W m^{-2} near 30°N (Fig. 5c). The corresponding vorticity forcing is negative, with a maximum intensity of -3×10^{-10} s^{-2} located at about 35°N (Fig. 5d). At 500 hPa, the vorticity advection ($-\boldsymbol{V}\cdot\nabla\zeta$) is of positive sign with an intensity of 1.5–2.0$\times10^{-10}$ s^{-2} above the surface forcing (Fig. 5e), and several times greater than the term $-\beta v$ (Fig. 5f). It is evident that the horizontal vorticity advection is a dominant factor in balancing the external vorticity forcing along the subtropics at middle levels. As a whole, the general features observed from panels (Fig. 5a) to (Fig. 5f) are similar to those shown in the schematic diagram Fig. 4a, indicating the possible linkage between surface sensible heating and the formation of the subtropical anticyclone via the β–effect and vorticity advection.

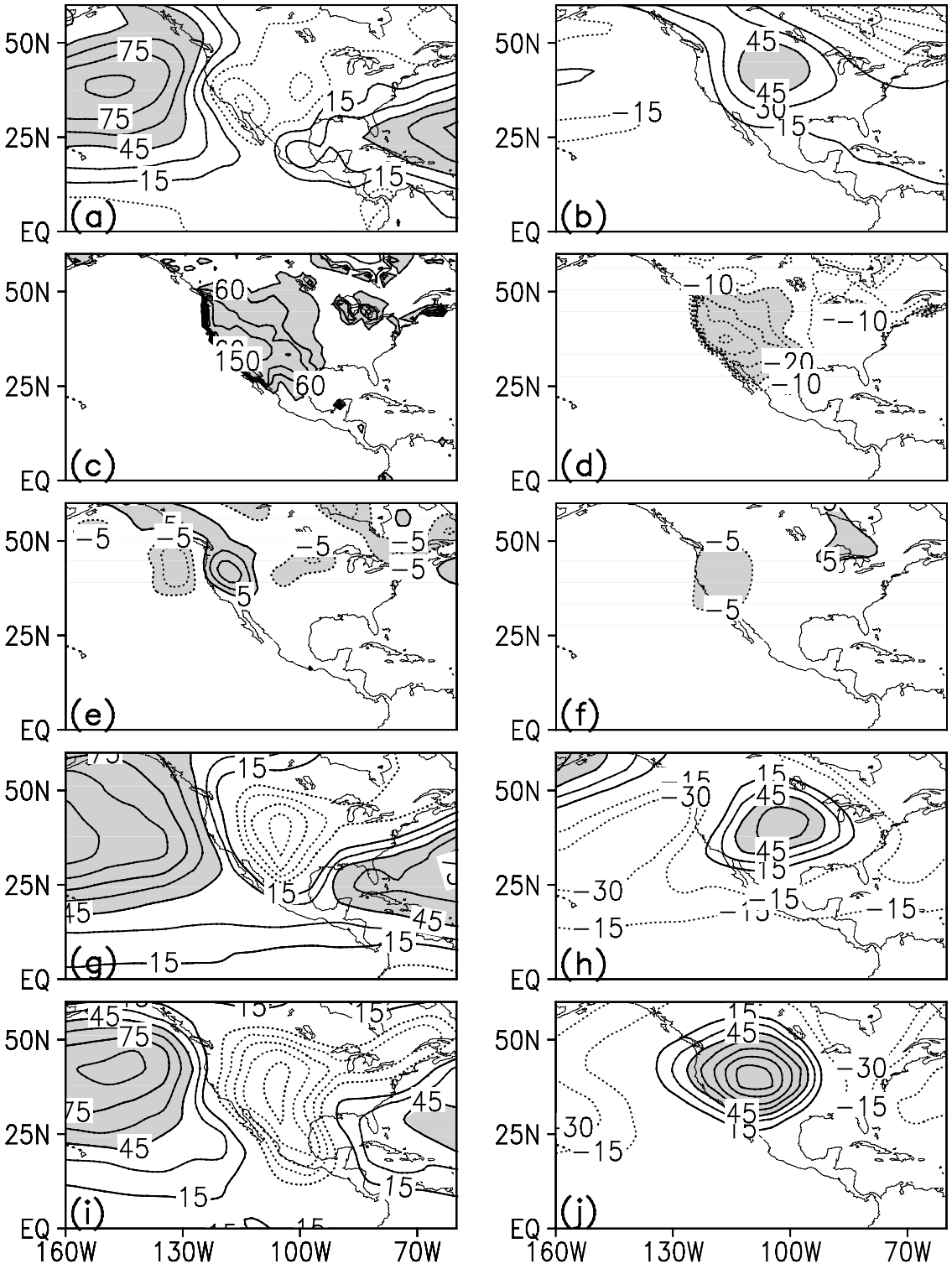

Fig. 5. Distributions of July means calculated from the NCEP/NCAR reanalysis of the zonal deviation of geopotential height (gpm) at (a) 1000 hPa and (b) 500 hPa, (c) surface sensible heat flux (W m^{-2}), (d) vorticity forcing (10^{-11} s^{-2}), and vorticity advection at 500 hPa (10^{-11} s^{-2}) of (e) $-\boldsymbol{V}\cdot\nabla\zeta$ and (f) $-\beta v$. The zonal deviations of geopotential height (gpm) obtained from the GCM experiment SH-1 are shown in (g) for 1000 hPa and (h) for 500 hPa. Those obtained from the GCM experiment SH-2 are shown in (i) for 1000 hPa and (j) for 500 hPa. (adopted from Wu et al., 2000)

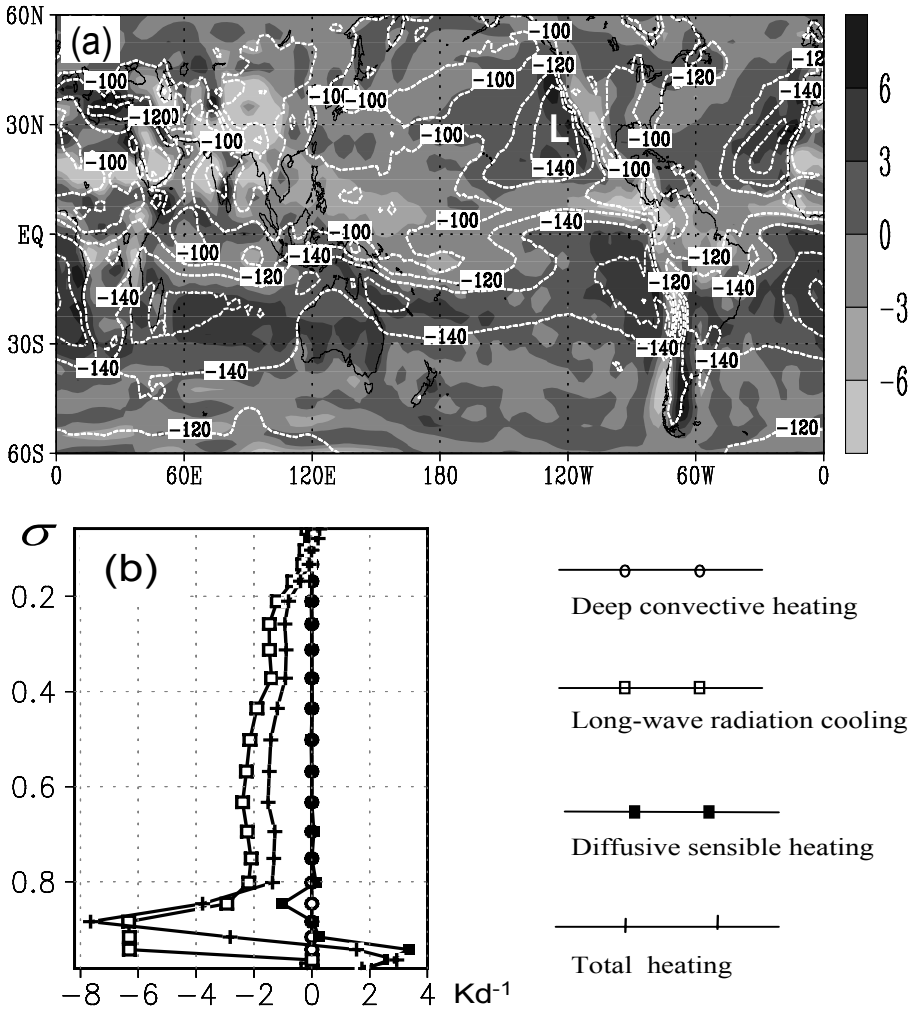

Fig. 6. (a) The July means averaged from1980 to 1997 of the total column integrated shortwave and longwave radiative heating rate (contours, units: W m^{-2}) and "vertical velocity" ω at 850 hPa (shading, units: 10^{-2} hPa s^{-1}). (b) The vertical profiles of different kinds of heating at the site L (30°N, 122°W) as shown in (a).

The general distributions shown in panels (Fig. 5a) and (Fig. 5b) are well reproduced by the GOALS_AGCM (Liu et al., 1999a). To verify further the impacts of the surface sensible heating on the subtropical anticyclone, a pair of numerical experiments is designed. To focus on land surface processes, the ocean component is switched off and replaced by the AMIP forcing for sea surface temperature and sea ice, which are based on observations and possess only the seasonal cycle. Then the model is integrated for 12 model years. Results from the last 10 years are extracted for analysis and defined as the Climate (CLI) run. The second numerical experiment is similar to the CLI run except it experiences the removal of the surface sensible heat flux throughout the experiment, and is defined as the no-sensible-heat flux (nSH) run. The summer rainfall in the subtropical region over Northwestern America is limited in both the CLI run and the nSH run (Liu, 1998), and the difference in rainfall over the area between CLI and nSH is not significant. Therefore, the differences between the two runs can be considered as the result of the surface sensible heating. Panels (g) and (h) of Fig. 5 show the distributions of geopotential height difference between CLI and nSH at 1000 hPa and 500 hPa, respectively. These are close to the observations shown in Fig. 5a and 5b and the corresponding model simulations, and are in good agreement with the schematic diagram shown in Fig. 4a. We can therefore reach the conclusion that the distribution of the subtropical anticyclone over the North Pacific (SANP) and North America in summer is, to a substantial extent, forced by the land-surface sensible

heating over the North American continent.

The main discrepancy between observation (Fig. 5a) and experiment (g) exists in the longitude location of the anticyclone center: in the experiment the center is shifted towards the dateline, whereas in the observation it is closer to the western coast of North America. This is because in such an experiment design, the impacts of radiation cooling are excluded, which will be further explored in section 5.

5. Radiative cooling and the subtropical anticyclone

Shortwave and longwave radiation fluxes penetrate the top and bottom surfaces of an atmospheric layer, and the convergence of these fluxes results in the warming or cooling of the bounded layer. In contrast with shortwave radiation, longwave radiation always cools the atmospheric column, and is strongly asymmetrically distributed particularly along the subtropics in the summer hemisphere. The distributions of total radiation heating, i.e., the sum of shortwave and longwave radiations are shown in Fig. 6a. They are negative everywhere, and the patterns resemble those of longwave radiation cooling. The belt of cooling of more than 140 W m^{-2} meanders around the tropics and subtropics in the Southern Hemisphere. In the Northern Hemisphere, such strong cooling is confined only to the eastern Pacific and Atlantic Oceans and North Africa.

The vertical profiles of different kinds of heating over the eastern Pacific (Fig. 6b) show that strong longwave radiation cooling of –6.5 K d^{-1} appears in the layer between 0.5 to 1.5 km (σ ~0.85 to 0.95) above sea level, in correspondence with the existence of the in situ low stratus clouds (Rodwell and Hoskins, 2001). The profile of total heating resembles the profiles of the longwave radiation cooling, with the maximum cooling near 1.5 km altitude. Since the total heating decreases with altitude below this level, but increases with altitude above this level, based on (9), the strong anticyclonic northerly near the surface and the southerly in the upper troposphere are then forced.

In Fig. 5g, although the surface sensible heating over the continents can generate the surface anticyclones over the ocean sectors, the center of the anticyclone over the North Pacific is shifted to the central Pacific compared with the observations (Fig. 5a). This may be due to the lack of radiative cooling over the eastern North Pacific in this experiment according to the above discussions. To verify this hypothesis, another experiment is designed. It is similar to the climate run CLI but with the removal of latent heating in the thermodynamic equation, and labeled as SH-2. It can be considered as the atmospheric response to surface sensible heating and radiative cooling. As shown in Figs. 5i and 5j, the zonal asymmetry of the surface oceanic anticyclone appears, and the simulated surface subtropical circulation (Fig. 5i) is closer to that in CLI. The forced anticyclone over North America is too strong because the model generates too strong sensible heating over the eastern part of North America. The anticyclone center over the North Pacific is located at 145°W both in SH-2 and in CLI, in agreement with the observations (Fig. 5a). Results from the above experiments then prove that it is mainly the radiative cooling over the eastern oceans that changes the symmetric surface anticyclones over the oceans into asymmetric ones, and shifts their centers eastward towards the western coasts of the continents.

For comparison, the field of "vertical motion" at 850 hPa is also plotted in Fig. 6a. It is clear that strong descent at the top of and within the planetary boundary layer is usually accompanied with the strong total column radiation cooling and in coordination with the ridgeline of the surface subtropical anticyclone. This is the same as the case along 125°W (Fig. 2b), and can also be interpreted by the frictional impacts within the planetary boundary layer. Such descent is to compensate for the cross isobaric divergence at the ridgeline of the subtropical anticyclone, and does not contribute to the in situ mass build up.

The distribution of the vertical velocity at 850 hPa is in general similar to that at 500 hPa. The main discrepancy exists over the western oceans in the Northern Hemisphere. Over the western Pacific, although the SAWP at 500 hPa is dominated by ascent (refer to Fig. 4b in Liu and Wu, 2000), the ridgeline of the surface subtropical anticyclone is characterized by near surface descent. Since most of the water vapor in the atmosphere is concentrated in the surface layer, the lower layer descent decreases the atmospheric relative humidity and prohibits the convergence of water vapor in the layer, leading to less cloud formation. This is why the approaching of a lower layer subtropical anticyclone is usually accompanied with clear sky.

6. Condensation heating and the subtropical anticyclone

In the boreal summer, the atmospheric circulation over East Asia is characterized by the existence of two persistent subtropical anticyclone systems. One is the pronounced South Asian High (SAH) in the upper troposphere just over the region to the north of the Bay of Bengal; and the other is SAWP. After early spring, the strong elevated surface sensible heating of the Tibetan Plateau persistently warms up the air column

aloft at a rate of 2°C to 4°C per day (Ye and Gao, 1979; Wu and Zhang, 1998; Wu et al., 1997a). These together with its mechanical forcing are essential in maintaining the huge upper layer anticyclone with a warm and moist core (Ye et al., 1957; Flohn, 1957; Ye and Wu, 1998). However, the anticyclone in the upper troposphere generated in such a way is mainly over the Plateau. Its location is somewhat to the north of the SAH center. It accounts for only a part of the formation of the SAH. On the other hand, the numerical experiment results of Li and Luo (1988) show that the moisture processes can enhance the SAH and the development of meridional flow. These provide the evidence that there must exist another mechanism that links the formation and maintenance of the SAH to the condensation heating in the monsoon area. Seeking for such a mechanism is the subject of the current section.

Most of the studies on the SAWP at 500 hPa were devoted to its impacts on the surrounding weather and climate (e.g., Huang and Yu, 1962; Tao and Chen, 1987; Samel et al., 1999). Nitta (1987) and Huang and Lu (1989) showed that, during the northward propagation of quasi-stationary planetary waves from a heat source near the Philippines, the SAWP shifts northward and intensifies. Despite these great efforts, the mechanism of the formation of the SAWP and its anomaly is still unclear in general. It is, however, interesting to notice that the movement of the SAH and that of the SAWP are not separated (Tao and Zhu, 1964). This then suggests the existence of some common mechanism that links the movement of one system to the other.

6.1 *Responses of the zonal symmetric circulation to an idealized latent heating*

For this purpose, the GOALS_AGCM is employed again to conduct a series of numerical experiments. To better understand the atmospheric response to condensation heating, an idealized "monsoon" heating (Fig. 7) is introduced into an aqua-planet. The condensation heating generated by the model and the global surface sensible heating, which will be diffused into the free atmosphere, have been turned off in the thermodynamic equation. The solar angle is fixed at its value on 15 July, and only the symmetric climate forcing is allowed. This perpetual July experiment is run for 24 months in total and is defined as experiment LH1 in the following contexts.

The outputs derived from the last 12 months' integration of LH1 are averaged and shown in Fig. 7. At the upper troposphere levels (Figs. 7a and b), high pressure appears on the western side of the heating source, and low pressure appears on its eastern side. At the lower troposphere level (Fig. 7c), the pressure pattern is reversed. The vertical distribution of the stream function (Fig. 7d) is in good agreement with the above theoretical analysis: it is due to the vertical gradient of condensation heating that the forced circulation displays a reverse phase between the upper and lower troposphere, namely, positive deviation appears to the west of the heating region in the upper troposphere, but to its east in the lower troposphere.

6.2 *Responses of the zonal symmetric circulation to the 'real' latent heating with and without orography*

The above results show that the subtropical anticyclones can result from an idealized condensation heating at the subtropics. To make the study more close to reality, in this section a prescribed grid-point forcing field for the July condensation latent heating is derived from the control experiment (CLI run in section 4). This forcing is considered as a 'real model heating', and the atmospheric response to the forcing is investigated in the following experiments.

Two perpetual July experiments, LH2 (without orography) and LH3 (with orography), are designed for the present purpose. The steady responses of geopotential heights in LH2 (Fig. 8a) are similar to those in LH1 (Fig. 7d). It is clear that the prescribed July condensation heating can break the zonal symmetric anticyclone belts into isolated anticyclones and cyclones. It contributes to the formation of the SAH and the tropical upper-tropospheric trough (TUTT) in the upper troposphere (200 hPa) and the SAWP in the middle troposphere (500 hPa).

The height deviation and condensation heating in LH3 shown in Fig. 8b indicate that, with orography and land-sea distribution included, the subtropical anticyclone in the middle and lower troposphere and the SAH in the upper troposphere can be produced to a reasonable extent. Comparing Fig. 8b with Fig. 8a, we see that the inclusion of the mechanical forcing of the Tibetan Plateau in LH3 causes the subtropical anticyclone at 200 hPa to be shifted westward to approach the observation site, just in phase with the plateau.

For comparison purposes, the vertical cross section along 30°N of the geopotential height deviations from zonal means calculated from the NCEP/NCAR reanalysis data is given in Fig. 8e. The strength of the SAH at 200 hPa is 100 to 120 gpm, and that of the SAWP in the middle troposphere (500 hPa) is less than 20 gpm. Near the surface, the center of the SANP is 90 gpm. In LH3 (Fig. 8b), the SAH center is only 60 gpm. The SAWP strength is as high as 40 gpm at 500 hPa. The

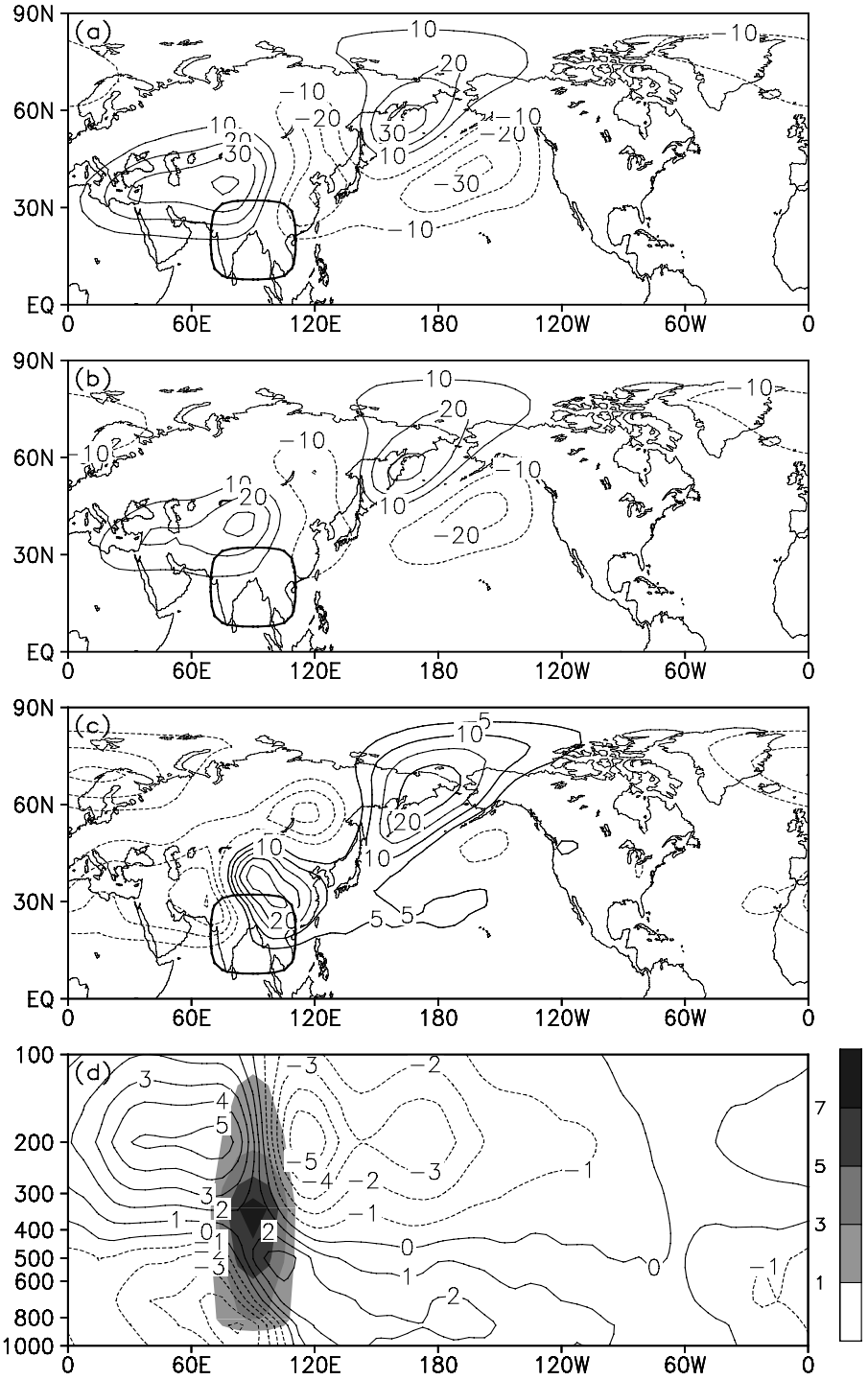

Fig. 7. Average fields of the last 12-month results from the idealized experiment LH1. (a)–(c): deviation of geopotential height from zonal mean at 200, 300, and 500 hPa, respectively. The contour interval is 10 gpm in (a) and (b), and 5 gpm in (c). The boxes bound the heating region which is more than 1 K d^{-1} at the level $\sigma = 0.336$. (d) Vertical cross-section of the stream function at 30°N, contour interval is 1×10^{-6} m^2 s^{-1}. The shaded area in d displays the profile of condensation heating at 20°N, and the contours denote 1, 3, 5, and 7 K d^{-1}, respectively. (adopted from Liu et al., 2001)

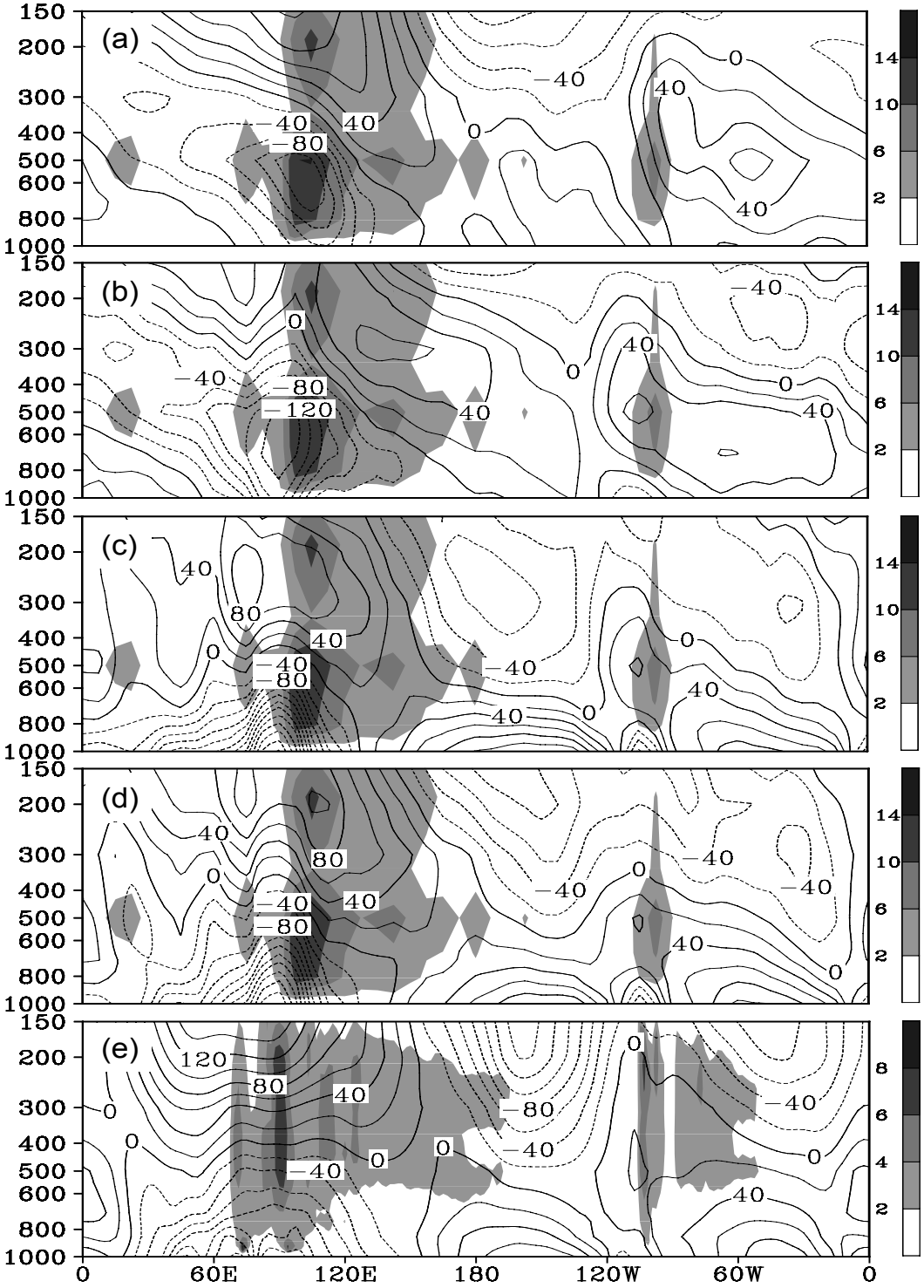

Fig. 8. Vertical cross-sections of the condensation heating (shaded) at 20°N in July and the corresponding geopotential height deviation from the zonal mean at 30°N (curves) averaged from the last 12-month results of experiments (a) LH2, (b) LH3, and (c) SHLH, (d) from the 16-year average of CLI, and (e) from the NCEP/NCAR reanalysis for 1980–95. Contour interval is 20 gpm. The boundaries of the shading present, respectively, the heating rates of 2, 6, 10, and 14 K d^{-1} in (a)–(d), and 2, 4, 6, and 8 K d^{-1} in (e). (adopted from Liu et al., 2001)

strength of the SANP is less than 20 gpm. Thus in LH3, the forced SAH and SANP are too weak, and the SAWP is too strong. There must exist a mechanism by which the SAH and SANP can be strengthened and the SAWP weakened.

6.3 *Influences of surface sensible heating and seasonal cycle*

According to the studies of Wu et al. (1997a), Wu and Zhang (1998), and Ye and Wu (1998), the surface sensible heating in summer over the Tibetan Plateau is a key factor to the formation of the anticyclone over the plateau. The results of section 4 also show that sensible heating is very important for the formation of the SANP.

Since in the lower troposphere the geopotential height deviation forced by sensible heating is out of phase with that forced by condensation heating, the too strong SAWP at 500 hPa and too weak SANP near the surface in LH3 must be due to the exclusion of the effects of sensible heating. In the next experiment, LHSH (Fig. 8c), besides the same orography and latent heating as in LH3, surface sensible heating and the associated vertical diffusive heating are also turned on. Comparing Fig. 8c with Fig. 8b, we see that sensible heating strengthens the SAH in the upper troposphere. This indicates that both the land surface sensible heating and condensation heating are important to the nature of the SAH. In the middle troposphere, sensible heating reduces the geopotential height over the oceans and weakens the SAWP. Near surface, it greatly intensifies the SANP and the subtropical anticyclone over the North Atlantic. Consequently, the cross section of the circulation pattern shown in Fig. 8c is closer to that from the reanalysis data (Fig. 8e).

All these experiments are perpetual July experiments. To see how the seasonal cycle affects the atmospheric responses, the results from the CLI are also presented in Fig. 8d. Its general features agree well with those presented in Figs. 8a to 8c. The use of perpetual experiments in understanding the mechanism of the subtropical anticyclone formation is validated. The effects of seasonal variation are to weaken the pressure systems in the lower troposphere and to strengthen the systems in the upper troposphere (CLI run, Fig. 8d). Therefore, the simulated circulation in CLI is much closer to the observations shown in Fig. 8e.

7. Mosaics of the heating quadruplet and circulation patterns

All of the above results indicate that different diabatic heatings play different roles in influencing the subtropical circulation. However, in the real atmosphere such individual thermal forcings are not isolated. Instead, they are well organized. To understand the formation of the subtropical anticyclones, they should be considered in synthesis (Wu and Liu, 2003). In this regard, the present section employs the reanalysis data of NCEP/NCAR from 1980 to 1997 to demonstrate the distributions of individual as well as total diabatic heating against circulations in the summer subtropics.

7.1 *Quadruple heating patterns*

In the northern subtropics there are two big continents. By selecting 150°W and 40°W as boundaries, the subtropical area can be divided to two regions, namely, the eastern North Pacific, North America, and the western North Atlantic region (PNAA); and the Atlantic- Africa- Eurasia- Pacific region (AAEP). Despite the huge area occupied by AAEP, it is shown that a quadruple heating pattern is found over each subtropical continent and its adjacent oceans (Figs. 9a and 9b). The ocean region to the west is characterized by strong LO; the western and eastern portions of the continent are dominated by sensible heating (SE) and condensation heating (CO), respectively; and the ocean region to the east is characterized by double dominant heating (D), with LO prevailing over CO. These compose a LOSECOD heating quadruplet. Its general feature is heating over the continent and cooling over the oceans. Since the heating quadruplet is mainly forced by the land distribution, the lateral boundaries of the mosaics are chosen at the longitudes over the oceans where SH is negligible and the surface meridional wind components vanish.

7.2 *Mosaics of circulation patterns*

Along the subtropics over PNAA or AAEP, the circulation pattern is well coordinated with the LOSECOD quadruplet. The continental area where the SE and CO heating prevail is characterized by the existence of surface cyclonic and upper tropospheric anticyclonic circulations. In contrast, the oceanic area where LO prevails is characterized by the existence of surface anticyclonic and upper tropospheric cyclonic circulations. This can be understood through the PV-θ view presented in section 3, according to which a heating (cooling) can produce lower layer cyclonic (anticyclonic) vorticity and upper layer anticyclonic (cyclonic) vorticity (Hoskins, 1991; Wu and Liu, 2000). However, such anticyclonic circulations near the surface (Fig. 9d) are strongly asymmetric about their central meridional axis. That is, over the LO lobe, the equatorward flow is strongly developed, whereas over

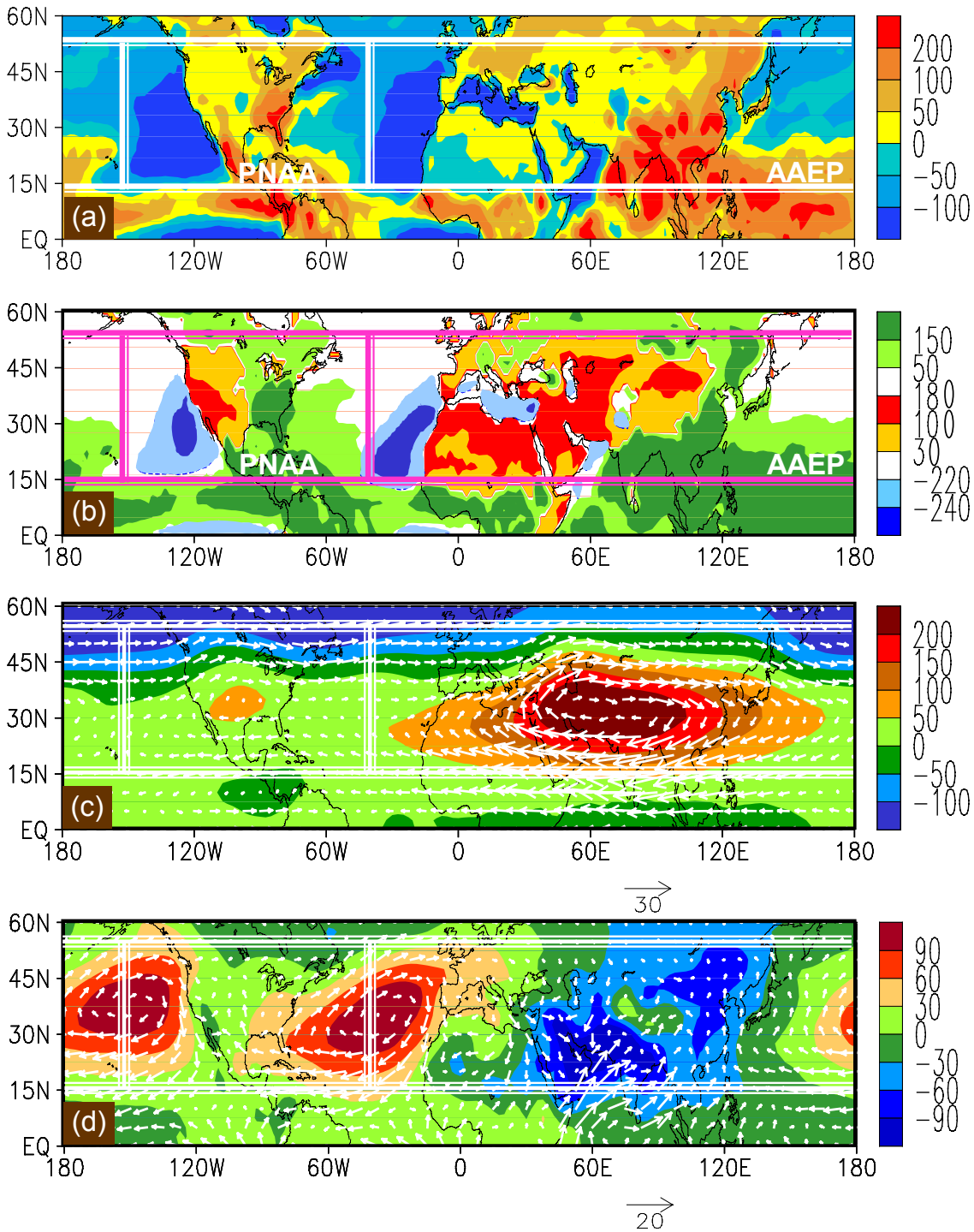

Fig. 9. July-mean distributions in the Northern Hemisphere of total column heating (a) and main local heating (b) in units of W m^{-2}, and the wind vector and deviation of geopotential height from the equatorial zonal-mean at 100 hPa (c) and 1000 hPa (d) with units of gpm. The heating distributions in the subtropics (a and b) demonstrate a mosaic of the quadruple LOSECOD heating pattern over the PNAA and AAEA regions. The circulations along the subtropics (c and d) also demonstrate a mosaic of the specific circulation pattern over the two regions. In (b), the blue color denotes longwave radiative cooling; yellow and red, sensible heating; and green, condensation heating. (adopted from Wu and Liu, 2003)

the D lobe, a band of southwesterly wind extends northeastward, just in coordination with the band of deep condensation heating over the western Pacific and the Atlantic (Fig. 9b). The correspondence between the profile of heating Q and meridional wind v can be interpreted by employing the Sverdrup balance Eq. (9). Since the total heating in the LO and SE lobes decreases with height rapidly in the lower layer, but increases with height in the deep upper layer (similar to Fig. 3a and Fig. 8b), the in situ strong near-surface equatorward flow and weaker upper-layer poleward flow should be generated, as demonstrated in Fig. 9d. A similar argument applies in the CO and D lobes where the total heating increases with height in the lower troposphere and decreases with height in the upper troposphere. Southerlies in the lower layers and northerlies in the upper layer are then observed.

At 100 hPa, in correlation with the vast longitude-span of the SE and CO lobes, the anticyclone covers the whole AAEP domain with a deviation height about three times as strong as its counterpart over PNAA. This is because in the absence of advection, the intensity of the geopotential height of a forced cyclone/anticyclone is proportional to the strength and the squared zonal half-length of the forcing. Furthermore, when the circulation patterns over AAEP and PNAA are placed side by side, the two troughs at 100 hPa and the two strong subtropical anticyclones at 1000 hPa appear just at the joined edges. It becomes apparent that for each strong oceanic surface subtropical anticyclone, its eastern part is substantially affected by radiative cooling and continental sensible heating, whereas its western part is to a great extent affected by radiative cooling as well as condensation heating associated with the summer monsoon.

In the southern subtropics there are three continents. In January, the longitude spans of the individual heating patterns in the southern subtropics differ very little from each other. Therefore the intensities of the three upper tropospheric anticyclones are similar. The mosaics of the three heating and circulation patterns are similar to what is observed in the Northern Hemisphere (Fig. 4 in Wu and Liu, 2003).

8. Concluding remarks

It has long been considered that the subtropical anticyclone is a result of the atmospheric descent, and is a giant master that controls the movement of the surrounding weather systems such as typhoons, fronts, torrential rains, and westerly troughs. Through theoretical investigation, data diagnosis, and numerical experiments, our studies show that the atmospheric descent cannot be used as a mechanism to interpret the formation of the summertime subtropical anticyclones. These are in fact forced basically by diabatic forcing.

In summertime, diabatic heating along the subtropics plays fundamental roles in the formation of the subtropical anticyclone. Strong surface sensible heating over the continents breaks the zonal symmetric subtropical anticyclone belt, forming surface lows over the continents and highs over oceans. Because the strong radiation cooling over the eastern oceans produces anticyclonic vorticity and a strong northerly near the surface, the center of the oceanic subtropical anticyclone is shifted eastward towards the western coast of the continent. On the other hand, the latent heat release of the Asian summer monsoon contributes substantially to the formation of the South Asian High in the upper troposphere and the anticyclone over the western Pacific in the middle and lower troposphere. The orographic forcing of the Tibetan Plateau and the surface sensible heating over the land surface also have strong impacts on their locations and intensities. The studies on the distributions of individual as well as total diabatic heating against circulations in the summer subtropics demonstrate that, over each continent and its adjacent oceans in the summer subtropics, there exist a heating quadruplet LOSECOD and an associated circulation pattern with surface cyclonic and upper-layer anticyclonic circulations over the continent but surface anticyclonic and upper-layer cyclonic circulations over the oceans, and the summer subtropical circulations can be viewed as a mosaic of such circulation patterns.

In some studies, the subtropical anticyclone over the western Pacific (SAWP) and the SANP near the surface are regarded as one circulation system (e.g., Yu and Wang, 1989). In these studies the SAWP is considered as the westward extension of the SANP, and its movement is forecasted by tracing the variations of the SANP. However, this study shows that their formation mechanisms are different. The SANP is forced dominantly by the land surface sensible heating over North America, whereas the SAWP is mainly by the monsoon condensation heating. They cannot be treated as one system.

The finding that the Asian monsoon rainfall can significantly affect the formation of the subtropical anticyclone over the western Pacific is of great importance. It raises an urgent need for change in methodology of short-term climate prediction. For many decades in meteorology, people predict the behavior of the subtropical anticyclone over the northwestern Pacific in summer months by using different statistical means and data collected several months before, then

the prediction of a distribution of rainfall anomalies is induced. Results from this study indicate that this method is inadequate, because it uses a false cause-effect relationship between rainfall and the variation of the subtropical anticyclone. For the prediction of the anomalous monsoon rainfall, we have to seek for other external forcing mechanisms, such as sea surface temperature anomalies in some oceanic regions, the Eurasian snow cover in winter months, and the thermal status of the Tibetan Plateau, etc. Continuous efforts oriented in this direction will lead us to better climate prediction in the future.

The discussions presented in this paper concentrate on the climate timescale. The short-term variation of the subtropical anticyclone is more complicated, and the interaction between the subtropical anticyclone and the surrounding weather systems (Wang et al., 2000; Lu, 2001; Lu and Dong, 2001) as well as global circulation adjustment should be considered. In addition, the latitude along $u = 0$ is the so-called critical latitude in wave dynamics. Here the southward propagating waves are absorbed, reflected, or trapped, behaving in a very complicated and highly nonlinear way. Such wave activity can alter the correlation between u and v and affect the transport of transient momentum, and thus change the time-mean strength of the westerlies. Such strong nonlinear activities are also important to the formation of the weather and climate patterns, and require further study.

Acknowledgments. This work was jointly supported by the Chinese Academy of Sciences (Grant No. ZKCX2-SW-210) and the Excellent Ph. D. Dissertation Award, and by the National Natural Science Foundation of China (Grant Nos. 40135020, 40221503, and 40023001).

REFERENCES

Bolin, B., 1950: On the influence of the earth's orography on the general character of the westerlies. *Tellus*, **2**, 184–195.

Charney, J. G., and A. Ellassen, 1949: A numerical method for predicting the perturbations of the middle-latitude westerlies. *Tellus*, **1**, 38–54.

Eady, E. T., 1949: Long waves and cyclone waves. *Tellus,* **1,** 33–52.

Flohn, H., 1957: Large-scale aspects of the "summer monsoon" in South and East Asia. *J. Meteor. Soc. Japan, 75th Ann. Vol.*, 180–186.

Haynes, P. H., and M. E. McIntyre, 1987: On the evolution of vorticity and potential vorticity in the presence of diabatic heating and frictional or other forces. *J. Atmos. Sci.*, **44**(5), 828–841.

Held, I. M., and A. Y. Hou, 1980: Nonlinear axially symmetric circulations in a nearly inviscid atmosphere. *J. Atmos. Sci.*, **37**, 515–533.

Hoskins, B. J., 1991: Towards a PV-θ view of the general circulation. *Tellus.* **43AB**, 27–35.

Hoskins, B. J., 1996: On the existence and strength of the summer subtropical anticyclones. *Bull. Amer. Meteor. Soc.,* **77**, 1287–1292.

Huang Shisong, 1963: Longitudinal movement of the subtropical anticyclone and its prediction. *Acta Meteorologica Sinica,* **33**(3), 320–332.

Huang Shisong, and Yu Zhihao, 1962: On the structure of the subtropical highs and same associated aspects of the general circulation of atmosphere. *Acta Meteorologica Sinica*, **31**, 339–359.

Huang Ronghui, and Li Lu, 1989: Numerical simulation of the relationship between the anomaly of the subtropical high over East Asia and the convective activities in the western tropical Pacific. *Adv. Atmos. Sci.*, **6**, 202–214.

IPCC, 2001: Chap. 8, Model evaluation. *Climate Change 2001: The Scientific Basis.* J. T. Houghton et al., Eds., Cambridge University Press, Cambridge and New York, 471–523.

Kalnay, E., and Coauthors, 1996: The NCEP/NCAR 40-year reanalysis project. *Bull. Amer. Meteor. Soc.,* **77**, 437–471.

Krishnamurti, T. N., S. M. Daggupaty, J. Fein, M. Kanamitsu, and J. D. Lee, 1973: Tibetan high and upper tropospheric tropical circulations during northern summer. *Bull. Amer. Meteor. Soc.*, **54**, 1234–1249.

Kuo, H. L., 1956: Forced and free meridional circulations in the atmosphere. *J. Meteor.,* **13**, 561–568.

Kurihara, K., 1989: A climatological study on the relationship between the Japanese summer weather and the subtropical high in the western northern Pacific. *Geophys. Mag.*, **43**, 45–104.

Kurihara, K., and T. Tsuyuki, 1987: Development of the barotropic high around Japan and its association with Rossby wave-like propagations over the North Pacific: Analysis of August 1984. *J. Meteor. Soc. Japan*, **65**, 237–246.

Li Maichun, and Luo Zhexian, 1988: Effects of moist process on subtropical flow patterns and multiple equilibrium states. *Scinices Sinica* (*B*), **31**(11), 1352–1361.

Liu Hui, and Wu Guoxiong, 1997: Impacts of land surface on climate of July and onset of summer monsoon: A study with an AGCM plus SsiB. *Adv. Atmos. Sci.*, **14**, 289–308.

Liu Ping, 1999: Interannual variations of the zonal mean subtropical anticyclone and the subtropical anticyclone over western Pacific and their association with the anomaly in sea surface temperature. Ph. D. dissertation, Institute of Atmospheric Physics, Chinese Acadeny of Sciences, 166pp.

Liu Yimin, 1998: Impacts of spatially non-uniform diabatic heating on the formation of subtropical anticyclone in boreal summer. Ph. D. dissertation, Institute of Atmospheric Physics, Chinese Acadeny of Sciences, 135pp. (in Chinese)

Liu Yimin, and Wu Guoxiong, 2000: On the studies of subtropical anticyclones: A review. *Acta Meteorologica Sinica*, **58**(4), 500–512.

Liu Yimin, Liu Hui, Liu Ping, and Wu Guoxiong, 1999a: The effect of spatially non-uniform heating on the formation and variation of subtropical high. Part II: Land surface sensible heating and East Pacific-North America subtropical high. *Acta Meteorologica Scinices*, **57**, 385–396.

Liu Yimin, Wu Guoxiong, Liu Hui, and Liu Ping, 1999b: The effect of spatially non-uniform heating on the formation and variation of subtropical high. Part III: Condensation heating and South Asia high and western Pacific subtropical high. *Acta Meteorologica Sinica*, **57**, 525–538.

Liu Yimin, Wu Guoxiong, Liu Hui, and Liu Ping, 2001: Dynamical effects of condensation heating on the subtropical anticyclones in the Eastern Hemisphere. *Climate Dyn.*, **17**, 327–338.

Liu, Y. M., J. C. L. Chan, J. Y. Mao, and G. X. Wu, 2002: The role of Bay of Bengal convection in the onset of the 1998 South China Sea summer monsoon. *Mon. Wea. Rev.*, **130**, 2731–2744.

Lu, R. Y., 2001: Interannual variability of the summertime North Pacific subtropical high and its relation to atmospheric convection over the warm pool. *J. Meteor. Soc. Japan*, **79**, 771–783.

Lu, R. Y., and B. W. Dong, 2001: Westward extension of North Pacific Subtropical High in summer. *J. Meteor. Soc. Japan*, **79**, 1229–1241.

Nikaidou, Y., 1988: Effects of high SST anomaly over the tropical western Pacific on climates predicted in 4-month integrations of the global spectral model T42. *Research Activities in Atmosphere and Ocean Modeling*, G. J. Boer, Ed., WMO/ TD, **263**(7), 19–20.

Nikaidou, Y., 1989: The PJ-like north-south oscillations found in 4-month integrations of the global spectral model T42. *J. Meteor. Soc. Japan,* **67**, 687–604.

Nitta, T., 1987: Convective activities in the tropical western Pacific and their impact on the Northern Hemisphere summer circulation. *J. Meteor. Soc. Japan,* **65**, 373–390.

Mao Jiangyu, Wu Guoxiong, Liu Yimin, Liu Ping, and Li Weiping, 2002: Study on modal variation of subtropical high and its mechanism during seasonal transition. Part I: Climatological features of subtropical high structure. *Acta Meteorologica Sinica*, **60**(4), 400–408.

Qian Zhencheng, and Yu Shihua, 1991: Mid-term variation in condensation heating over East Asia and the quasi-two-week oscillation of the subtropical anticyclone over the western Pacific. *Trop. Meteor.*, **7**, 259–267.

Rodwell, M. R., and B. J. Hoskins, 2001: Subtropical anticyclones and monsoons. *J. Climate*, **14**, 3192–3211.

Samel, A. N., W. C. Wang, and X. Z. Liang, 1999: The monsoon rainfall over China and relationships with the Eurasian circulation. *J. Climate*, **12**, 115–131.

Shi Guangyu, 1981: An accurate calculation and the infrared transmission function of the atmospheric constituents. Ph. D. Dissertation, Tohoku University of Japan, 191pp.

Tao Shiyan, 1963: *On the Summer Synoptic Systems in the Subtropics over China*. Science Press, Beijing. (in Chinese)

Tao Shiyan, and Zhu Fukang, 1964: Variation of summer circulation pattern at 100 hPa over South Asia and its relation with the movement of the subtropical anticyclone over Western Pacific. *Acta Meteorologica Sinica,* **34**(4), 385–394.

Tao Shiyan, and Chen Longxun, 1987: A review of recent research on the East Asia summer monsoon in China. *Monsoon Meteorology*, Krishnamutri, Ed., Oxford University Press, 60–92.

Tao Shiyan, and Xue Shuying, 1962: Circulation characteristics in association with persistent summer drought and flood in the Yangtze-Huaihe River reaches. *Acta Meteorologica Sinica,* **32**(1), 1–18.

Tao Shiyan, Xue Shuying, and Guo Qiyun, 1962: Meridional and longitudinal circulation pattern in summer in the tropical and subtropical regions over East Asia. *Acta Meteorologica Sinica,* **32** (1), 91–102.

Wang, B., R. Wu, and X. Fu, 2000: Pacific–East Asian teleconnection: How does ENSO affect East Asian climate? *J. Climate*, **13**, 1517–1536.

Wu Guoxiong, 1988: Roles of the mean meridional circulation on atmospheric budgets of angular momentum and sensible heat. *Chinese J. Atmos. Sci.*, **12**, 11–24.

Wu Guoxiong, Liu Hui, Zhao Xueheng, and Li Weiping, 1996: A nine-layer atmospheric general circulation model and its performance. *Adv. Atmos. Sci.*, **13**, 1–18.

Wu Guoxiong, Li Weiping, Guo Hua, and Liu Hui, 1997a: Sensible heating-driving air pump of the Tibetan Plateau and the Asian summer monsoon. *Memorial Volume of Prof. Zhao Jiuzheng*, Ye Duzheng, Ed., Science Press, Beijing 116–126. (in Chinese)

Wu Guoxiong, Zhang Xuehong, Liu Hui, Yu Yongqiang, Jin Xiangzhe, Guo Yufu, Sun Shufen, and Li Weiping, 1997b: The LASG global ocean-atmosphere-land system model GOALS/LASG and its simulation study. *App. Meteor.*, **8**(spec.), 15–28. (in Chinese)

Wu Guoxiong, and Liu Yimin, 2000: Thermal adaptation, overshooting, dispersion, and subtropical anticyclone. I: Thermal adaptation and overshooting. *Chinese J. Atmos. Sci.*, **24**(4), 433–446.

Wu Guoxciong, and Liu Yimin, 2003: Summertime quadruplet heating pattern in the subtropics and the associated atmospheric circulation. *Geophys. Res. Lett.*, **30**(5), 1201–1204.

Wu Guoxciong, and Liu Yimin, Liu Ping, and Ren Rongcai, 2002: Relation between the zonal mean subtropical anticyclone and the sinking arm of the Hadley cell. *Acta Meteorologica Sinica,* **60**(5), 635–636.

Wu Guoxciong, Liu Yimin, and Liu Ping, 1999: Spatially inhomogeneous diabatic heating and its impacts on the formation and variation of subtropical anticyclone, I. Scale analysis. *Acta Meteorologica Sinica*, **57**(3), 257–263.

Wu Guoxciong, and Zhang Yongshen, 1998: Tibetan Plateau forcing and the timing of the monsoon onset over South Asia and the South China Sea. *Mon. Wea. Rev.*, **126**, 913–927.

Xue, Y. K., P. J. Sellers, J. L. Kinter, and J. Shukla, 1991: A simplified biosphere model for global climate studies. *J. Climate*, **4**, 345–364.

Ye Duzheng, and Zhu Baozhen, 1958: *Some Fundamental Problems of the General Circulation of the Atmosphere.* Science Press, Beijing, 159pp.

Ye Duzheng, and Wu Guoxciong, 1998: The role of the heat source of the Tibetan Plateau in the general circulation. *Meteor. Atmos. Phys.*, **67**, 181–198.

Ye Duzheng, Luo Siwei, and B. C. Chu, 1957: On the heat balance and circulation structure in the troposphere over the Tibetan Plateau and its vicinity. *Acta Meteorologica Sinica*, **28**, 108–121.

Ye Duzheng, Tao Siyan, and Li Maichun, 1958: Abrupt seasonal change of the general circulation in June and October. *Acta Meteorologica Sinica*, **29**, 249–263.

Ye Duzheng, and Gao Youxi, 1979: *Meteorology over the Tibetan Plateau.* Science Press, Beijing, 278pp.

Ye Duzheng, 1950: The circulation of high troposphere over China in winter of 1945–46. *Tellus*, **2**, 173–183.

Yu Shihua, and Wang Shaolong, 1989: Circulation mechanism leading to the mid-term variation of the subtropical anticyclone over western Pacific. *Acta Oceano. Sinica*, **11**(3), 370–377.

Zhang, X. H., K. M. Chen, X. Z. Jin, W. Y. Lin, and Y. Q. Yu, 1996: Simulation of thermohaline circulation with a twenty-layer oceanic general circulation model, *Theor. Appl. Climatol.,* **55**, 65–88.

Zhang Xuehong, Shi Guangyu, Liu Hui, and Yu Yongqiang, 2000: *IAP Global Ocean-Atmosphere-Land System Model.* Science Press, Beijing, New York, 252pp.